PHYSICAL REVIEW B

CONDENSED MATTER

THIRD SERIES, VOLUME 29, NUMBER 5 1 MARCH 1984

Variable-energy positron studies of metallic glasses

A. Vehanen,* K. G. Lynn, and Peter J. Schultz
Brookhaven National Laboratory, Upton, New York 11973

E. Cartier
Laboratorium für Festkörperphysik, Eidgenössische Technische Hochschule Zürich, CH-8093 Zürich, Switzerland

H.-J. Güntherodt
Institut für Physik, Universität Basel, CH-4056 Basel, Switzerland

D. M. Parkin
Los Alamos National Laboratory, Los Alamos, New Mexico 87545
(Received 20 July 1983)

The temperature dependence of the effective positron diffusion length L_+ has been studied in various metallic glasses with variable-energy positrons. All the initial measurements in the glasses show a very short diffusion length ($L_+ \approx 10$ Å) that is alloy dependent. This is more than 2 orders of magnitude smaller than L_+ in annealed crystalline metals, and is ascribed to positron trapping at a high concentration of intrinsic defects. Larger values of L_+ are found in the metal-metalloid than in the metal-metal glasses. This is suggested to be caused by boron filling some of the open-volume areas, thereby decreasing the positron trapping rate. Our results are compatible with a density of a few percent of point defects or, alternatively, about 10^{13} cm^{-2} of dislocation-type defects. Evidence was found on the existence of a nonhomogeneous defect profile in the near-surface region. Both reversible and irreversible changes in L_+ are observed during heating and cooling cycles, attributed to positron thermal detrapping and structural relaxation, respectively. Crystallization causes partial removal of the defect structure, but temperatures close to the melting point are required before positron trapping is significantly reduced. In $Gd_{67}Co_{33}$ positron localization remains even after annealing 50 °C below the melting point. The trapping behavior in this alloy was found to depend on specimen heating and cooling rates indicating an ongoing phase-segregation process. The data for L_+ are compared with previously obtained bulk angular correlation data as well as Doppler-broadening line-shape parameters to provide a consistent picture of the defects in these systems.

I. INTRODUCTION

Metallic glasses have become a subject of considerable interest in basic and applied research due to their unique physical and mechanical properties, e.g., high mechanical ductility and magnetic permeability, and resistance to corrosion and irradiation.[1] However, the theoretical description of the ionic structure is still incomplete and very little is known about the structure of defects, which strongly influence the mechanical behavior of crystalline metals.[2] In this paper we present results obtained with a variable-energy positron beam which illustrate several features of the defects in a variety of as-received and annealed metallic glasses.

Positrons implanted into a metal thermalize rapidly and tend to localize into regions of lower than average ionic density. Information about the structure and concentration of various crystal imperfections can be obtained from measurements of the annihilation radiation.[3] Such data have been obtained for various metallic glasses, but because the nature of the positron state is still not well understood, interpretation is somewhat uncertain (for recent reviews, see Refs. 4–6). Early bulk positron experiments showed very small changes in the annihilation characteristics upon crystallization.[7–10] ("Bulk" positron experiments, as opposed to "variable-energy experiments," are done employing isotopic sources rather than tunable beams.[3]) Room-temperature electron irradiation[11] or plastic deformation[12] also failed to induce detectable changes in the positron state. It was concluded that there were no

defects capable of positron localization both in the as-received state and after irradiation or deformation.

More recent data showed significant changes between various states of the sample. The line-shape parameter I_v describing the shape of the 511-keV annihilation line was markedly temperature dependent below room temperature leading to the conclusion that positrons were trapping at defects.[13] The smearing of the angular correlation of the annihilation-radiation curve at Fermi momentum was enhanced at low temperatures, attributed to positron trapping at low-density dilated regions of the amorphous structure.[14] Increased positron trapping was demonstrated following low-temperature electron irradiations[15,16] and the data indicated that positron localization into irradiation-induced defects competed with a high concentration of preexisting low-density regions inherently present in the amorphous state. Although in many cases the positron lifetime spectrum cannot be reliably decomposed into more than one exponential component, the combination of positron lifetime and angular correlation measurements[17] seem to indicate the presence of at least two different positron states. Thus the early view of a free Bloch-like positron state in metallic glasses was replaced by a model of 100% positron trapping into a spectrum of intrinsic defects.

Contrary to this prevailing view of complete positron localization, recent angular correlation measurements of Cartier *et al.* showed indications of a delocalized positron state in amorphous Cu-Zr (Ref. 18) and Ca-Mg glasses.[19] In addition, lifetime and Doppler-broadening measurements of Kögel and Triftshäuser in Ti-Be-Zr glasses[20] were interpreted in terms of positrons having only a low probability for localization. Thus some uncertainty about the nature of the positron state in amorphous metals still persists, which restricts the structural information obtainable by conventional positron-annihilation measurements. The possible states of positrons in metallic glasses—other than free Bloch-like and localized states encountered in crystalline metals—include (i) strong scattering of positrons from fixed scattering centers, (ii) positron trapping into low-binding-energy defects (and consequent thermal detrapping), and (iii) enhanced affinity of positrons into one type of atoms or clusters of atoms in the amorphous structure. In case of having an extremely high density of defects with a relatively low binding energy available for positron localization, the probability of positrons to tunnel from one defect to another might be high enough to significantly change the diffusion behavior of positrons. This would be the first example of interdefect tunneling processes.

Information about the diffusion properties of positrons can be deduced by utilizing a variable-energy positron beam[21] in ultrahigh vacuum conditions. Positrons with an incident energy (variable from 0 to a few keV) are implanted into the specimen, where they rapidly thermalize in the near-surface region (<1000 Å). They have an energy-dependent probability of diffusing back to the surface which is dependent on the implantation profile. This probability can be experimentally measured and analysis of the data (cf. Sec. III) yields the diffusion length of positrons

$$L_+ = (D_+ / \kappa_{\text{eff}})^{1/2} , \tag{1}$$

where D_+ is the positron diffusion coefficient and κ_{eff} is the net removal rate of positrons from the freely diffusing state. κ_{eff} depends on the annihilation, trapping, and detrapping rates of positrons from various states in the sample.[22]

In this paper we measure L_+ as a function of specimen temperature in various amorphous metals both below and above the crystallization temperature, T_c. Our results show an unusually low level of L_+ in all glasses in the as-received state at room temperature. This is ascribed to a high probability of positron trapping into defects present in the amorphous structure. No specific information on the nature of these defects is provided by the present experiments. Both compositional and topological disorder is expected to localize positrons with the latter likely being associated with a stronger positron binding. Evidence for positron thermal detrapping is also found, reflecting the fact that at least some of the defects localize the positron with a relatively low binding energy. In addition, irreversible changes of L_+ occur indicating the structural relaxation in the amorphous phase. Crystallization of the samples also changes L_+, but significant positron trapping remains until much higher temperature. In some crystallized glasses the defect structure anneals out close to the melting point of the alloy, although in others this is not the case. A preliminary report of some of the present results has been published.[23]

II. EXPERIMENTAL PROCEDURE

Five different samples were studied (typically 2×5 cm$\times40$ μm), two of which ($Fe_{40}Ni_{40}P_{14}B_6$ and $Fe_{82}B_{12}Si_6$) were obtained from commerical sources.[24] $Cu_{30}Zr_{70}$ and $Cu_{50}Zr_{50}$ alloys were prepared with splat cooling[25] and $Gd_{67}Co_{33}$ was made by the melt-spinning tecnhique[25] in a vacuum of about 10^{-7} Torr. Specimens from the same sources were used in conventional bulk positron experiments previously reported.[12,18,19,25] The measuring sequence was also done using similar heat-treatment cycles and heating rates as were used in the other experiments.[18,19,25] The samples were determined to be amorphous with x-ray diffraction. They were cleaned in an ultrasonic bath of acetone and ethyl alcohol and then mounted by spot welding onto Ta posts in a UHV sample holder.

The variable-energy positron apparatus used for the experiments has been described elsewhere.[26] The intensity of the positron beam (diameter ≈6 mm) impinging on the samples was typically 1×10^6 sec^{-1} and the incident energy range was from 25 eV to 7 keV (±1 eV). The base pressure throughout the measurements was $\approx1\times10^{-9}$ Torr. The sample surfaces were cleaned *in situ* by sputtering several hours with low energy (650 eV) Ar^+ ions using 5-μA beam current. This resulted in an estimated removal of 1—2 μm of the surface. Sputtering was performed because the probability of forming Ps at the surface (cf., Sec. III) was very small due to surface impurities, thus reducing the sensitivity of our measurements. The diffusion length L_+ in the as-received state was not affected by the sputtering process. For $Fe_{40}Ni_{40}P_{14}B_6$ samples we

measured the diffusion length both before and after Ar^+ sputtering and after chemical etching, and the results for the diffusion length were found to be in agreement. We also checked the possibility of inducing sputtering damage in the near-surface region by resputtering the samples after the final heat treatment. No changes could be observed in the L_+ due to this additional low-energy sputtering. A change was observed when the sputtering was done with 3-keV Ar^+ ions. The surface of the samples was checked periodically during the experiments with Auger electron spectroscopy. Submonolayer contamination of carbon, nitrogen, and oxygen was found, known to be bulk impurities in the samples. Specimen temperature was controlled by resistive heating of either the sample itself ($Fe_{40}Ni_{40}P_{14}B_6$ and $Fe_{82}B_{12}Si_6$) or a tantalum backing foil spot welded to the sample ($Cu_{30}Zr_{70}$, $Cu_{50}Zr_{50}$, and $Gd_{67}Co_{33}$). The experimental procedure for the angular correlation experiments has been described in detail in a previous publication.[18]

III. DATA ANALYSIS

Positrons implanted into a metal with an incident energy E, thermalize at mean depths of $x=AE^n$,[21] where the constants $A=3.3\ \mu g\,cm^2(keV)^{-n}$ and $n=1.4$–1.6 have been obtained from foil transmission measurements.[27] A diffusive motion through the metal then follows and eventually positrons annihilate either from the freely diffusing state or from a localized state with a characteristic lifetime of 100–500 psec.[3] With low enough incident energies positrons can also diffuse back to the surface. The predominating processes at the surface of metals then include: (i) direct positron reemission into the vacuum, provided that the positron work function ϕ_+ is negative,[28] (ii) direct positronium atom (Ps) emission into vacuum provided that the Ps work function ϕ_{Ps} is negative,[29,30] and (iii) localization into a surface state with possible thermal desorption into the vacuum as Ps at higher sample temperatures.[30]

For constant surface conditions of the specimen the emitted Ps fraction F is proportional to the probability of positrons diffusing back to the surface. This can be experimentally observed, since the triplet Ps decays predominantly by the emission of three photons having a continuous energy distribution rather than the exclusive 511-keV emission from "free" positron or singlet Ps decay. F is calculated from the shape of the energy distribution of annihilation quanta after calibrating with reference spectra with 0% and 100% Ps emission.[22] Assuming the structure of the sample is uniform over the full range of depths studied, and assuming an exponential positron implantation profile, F depends on the incident energy E as[21,22,31]

$$F(E)=\frac{F_0}{1+(E/E_0)^n}\ , \tag{2}$$

where F_0 is the surface-sensitive branching ratio of the back-diffused positrons to be emitted as Ps atoms into the vacuum. The diffusion length from Eq. (1) is related to the measurement, viz.,

$$L_+=(D_+/\kappa_{\rm eff})^{1/2}=AE_0^n\ . \tag{3}$$

In the general case of one free and N different localized states in the sample we have for the removal rate, $\kappa_{\rm eff}$:

$$\kappa_{\rm eff}=\lambda_{\rm free}+\sum_{i=1}^{N}\frac{\kappa_i}{1+\delta_i/\lambda_i}\ , \tag{4}$$

where $\lambda_{\rm free}$ and λ_i are the annihilation rates in the free and in the localized states, respectively, κ_i is the trapping rate proportional to the corresponding defect concentration, and δ_i is the thermal detrapping rate back into the freely diffusing state.

We have measured the diffusion length L_+ from the incident energy dependence of the Ps fraction F at a fixed specimen temperature. In some cases we ramped the temperature up or down slowly ($\Delta T/\Delta t\approx 0.5\,^\circ$C/min) as compared to the time required to complete a voltage cycle (≈ 11 min). At each temperature F was measured using (typically) 16 different voltages in random order, each of which required aobut 40 sec to yield a statistical precision in F of about 0.5%. Equation (2) was fitted to the experimental data with a nonlinear fitting procedure resulting in values of n ranging from $n=1.4$ to 1.7. For each sample we reanalyzed the data assuming the average value of $n\approx 1.6$.[31] The F_0 and E_0 values obtained in this way are presented and discussed throughout the next section.

IV. RESULTS AND DISCUSSION

A. Positron-surface interaction in amorphous metals

At room temperature the analyzed values of F_0 and E_0 have typical ranges of 0.4–0.7 and 250–500 eV, respectively. While the former is commonly observed for well-characterized surfaces of metal single crystals, E_0 is more than an order of magnitude smaller compared to E_0 usually observed for defect-free metals with similar mass densities.[21] F_0 increases both in a reversible and an irreversible manner as specimen temperature is increased, ascribed to enhanced positron thermal detrapping from the surface state[30] and changes in the surface structure, respectively. An example of the former is shown in Fig. 1, where the analyzed F_0 values are plotted as a function of temperature for a $Gd_{67}Co_{33}$ specimen which has been crystallized at 960 K. This behavior of F_0 is characteristic of thermal desorption observed for positrons at surfaces of metal single crystals. A fit of the temperature dependence of F_0 to the model[30–32] of detrapping yields a value for the activation energy $E_a=0.22\pm 0.04$ eV.

From the above we conclude that the positron-surface interaction is governed by the same processes as are found in well-characterized surfaces and the diffusion length L_+ (or E_0) measurements can be interpreted analogously to annealed or defected crystalline metals. On the other hand, the positron-lattice interaction is much stronger than what is observed in annealed metals suggesting that the positron state in metallic glasses is markedly different from the free Bloch state encountered in crystalline metals.

Evidence for positron reemission was sought using positron work-function measurements.[28] No reemission was found, suggesting that the work function was positive.

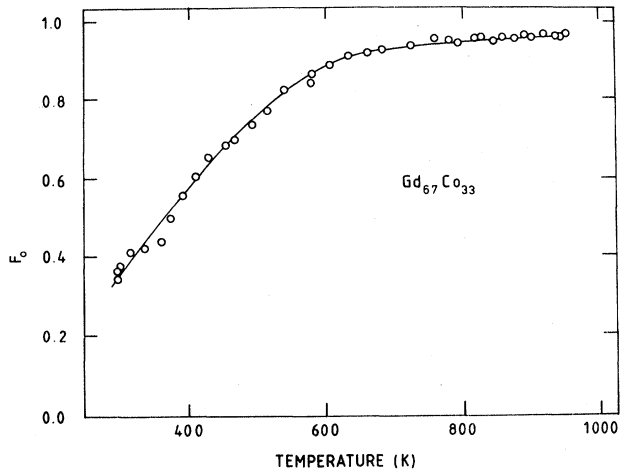

FIG. 1. The fitted parameter F_0 in Eq. (2) as a function of temperature in a $Gd_{67}Co_{33}$ alloy. The shape of F_0 is compatible with thermally activated detrapping of positrons from the surface state forming positronium with an activation energy of $E_a = 0.22 \pm 0.04$ eV.

This is not unusual, since a number of clean single-crystal surfaces also exhibit positive positron work functions.[21]

B. Diffusion length in $Fe_{82}B_{12}Si_6$ glass

Figure 2 shows the analyzed values of E_0 in the amorphous metal $Fe_{82}B_{12}Si_6$ at different sample temperatures. As discussed previously, $E_0 = 520 \pm 70$ eV (in the initial state) is significantly lower than that in defect-free crystalline metals (ranging from $E_0 \approx 3$ keV for Al to $E_0 > 15$ keV for W).[21] The corresponding diffusion length from Eq. (3) in $Fe_{82}B_{12}Si_6$ is about $L_+ \approx 15$ Å, which is a factor of 50—100 lower than that in crystalline metals. If we would assume that no positron localization occurs, we find [cf. Eq. (4)] $\kappa_{\text{eff}} = \lambda_{\text{free}} \approx 6 \times 10^9$ sec^{-1}.[4-6] Thus we obtain from Eq. (1) a value for $D_+ = 1.4 \times 10^{-4}$ cm^2/sec.

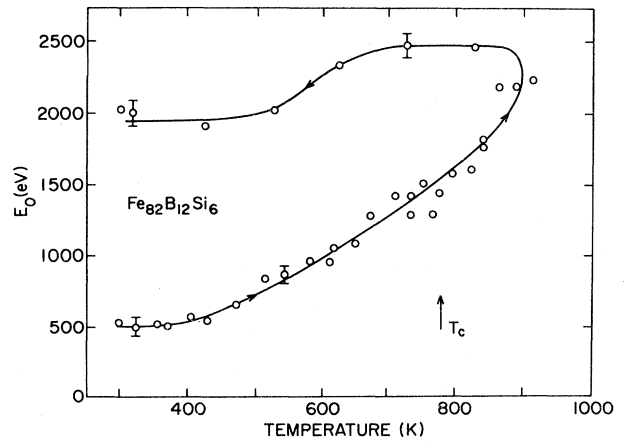

FIG. 2. The fitted values of E_0 in Eq. (2) are shown vs specimen temperature in amorphous $Fe_{82}B_{12}Si_6$. The arrows show the sequence of measurements. $T_c = 780$ K is the crystallization temperature. Very little hysteresis is observed up to 660 K, whereas annealing at 740 K changed the room-temperature value of E_0 to 1200 eV.

This is roughly 4 orders of magnitude less than what is found in most crystalline materials (see Ref. 33, and references therein). The low D_+ values may tentatively be explained by using the concept of a high positron scattering probability from structural inhomogeneities of the material (and the absence of trapping). However, the use of the standard model[34] of elastic "impurity" scattering of positrons leads to an unreasonable concentration of scattering centers. Assuming, for instance, that the positron band mass is $m^* = 1.5 m_e$, impurity-host pseudopotential difference $\Delta V = 2$ eV, and impurity cell radius $R_a = 3$ Å,[34] only an unphysical impurity concentration $c_{\text{imp}} \simeq 1.1 \times 10^{+4}$ is compatible with the low value of D_+. Moreover, the temperature dependence of E_0 in Fig. 2, which we observe to be very nearly reversible up to 620 K, is much stronger than the predicted impurity-dominated $T^{+0.5}$ dependence of D_+.[34] Our results thus rule out the possibility of a free Bloch-like positron state at room temperature in this glassy metal, indicating that positrons are strongly coupled to the inhomogeneities of the sample.

The obvious reason for the low E_0 values seems to be positron trapping into intrinsic defects in the material. Assuming the absence of positron detrapping from these defects at room temperature we obtain [cf. Eq. (4)] a lower limit for the total trapping rate $\kappa_{\text{eff}} \geq 1 \times 10^{12}$ sec^{-1}, where a reference value of $E_0 \cong 2500$ eV in a defect-free material has been used (see Fig. 2 and discussion below).[35]

The temperature dependence of E_0 above room temperature shows very little hysteresis up to 620 K, whereas after 740 K we measured $E_0 \approx 1200$ eV upon cooling back to room temperature (not shown in the figure). Thus structural changes occur in the amorphous phase between 620 and 740 K, which further supports our concept of positron trapping into defects in the amorphous structure. It also demonstrates that measurements of E_0 are sensitive to changes in the short-range order in the amorphous phase. Furthermore, the temperature dependence of trapping seems to be much stronger than what is observed in the case of point defects and dislocations in crystalline metals.[33] At higher temperatures the trapping probability decreases, which can be explained by thermal detrapping of positrons from the localized states.

During further heating we observe no abrupt changes in E_0 upon passing the crystallization temperature $T_c = 780$ K. The steady growth of E_0 towards a value of 2450 ± 80 eV continues up to 920 K, the maximum temperature used in the experiment. During subsequent cooling we observed a sigmoidal decrease of E_0 around 600 K and the room-temperature value is $E_0 = 2000 \pm 70$ eV. This suggests that positron trapping still persists in the crystallized alloy, and the remaining increase of E_0 at 600 K can be attributed to thermal detrapping of positrons from these localized states in the bulk. Thus the defect-free reference level for E_0 is at least 2.5 keV for $Fe_{82}B_{12}Si_6$ (see Table I).

C. Diffusion length in $Fe_{40}Ni_{40}P_{14}B_6$

Figure 3 displays the E_0 values measured as a function of specimen temperature for a $Fe_{40}Ni_{40}P_{14}B_6$ glass. For comparison the peak rate $\hat{N}$ of the angular correlation versus specimen temperature is shown in the upper part of

TABLE I. Values of E_0 and the corresponding positron diffusion lengths L_+ in various amorphous metals in the as-received and annealed states. Reference values of E_0 and L_+ in some annealed single-crystal metals are also given. κ_{eff} is the estimated lower limit of the total positron trapping rate into localized states in the as-received samples. Estimates are also given for the defect concentrations in the as-received state for three structural models.

Material	E_0 (eV) as-received	L_+ (Å) as-received	E_0 (eV) annealed	L_+ (Å) annealed	κ_{eff} (sec^{-1}) as-received	c_{vac} point defects	c_{disl} (cm^{-2}) line defects	$\bar{l}$ (Å) micrograins
$Fe_{82}B_{12}Si_6$	520±70	15±3	>2500	>180	$>1.0\times10^{12}$	>1%	$>10^{13}$	>450
$Fe_{40}Ni_{40}P_{14}B_6$	500±40	14±2	3000±130	260±20	2.5×10^{12}	2.5%	2.5×10^{13}	300
$Cu_{30}Zr_{70}$	280±40	6±1	3500±150	360±25	2.5×10^{13}	25%	2.5×10^{14}	90
$Cu_{50}Zr_{50}$	270±40	6±1	≈3500	≈360	$\approx2.8\times10^{13}$	≈28%	$\approx2.8\times10^{14}$	≈80
$Gd_{67}Co_{33}$	390±60	8±2	>2200	>120	$>1.5\times10^{12}$	>1.5%	$>1.5\times10^{13}$	380
Cu			8000	1050				
Ni			8300	1100				
Al			3200	800				
W			>15 000	>1300				

the figure. We note the qualitative similarity of these results with those shown in Fig. 2. The initial value for E_0 is 500±40 eV corresponding to $L_+\approx14$ Å (see Table I). However, it stays fairly constant up to 600 K. In this case L_+ does not seem to be sensitive to the observed[36] changes in the short-range order below 600 K. A gradual increase of the diffusion length occurs in the vicinity of crystallization at $T_c=650$ K (Ref. 37) consistent with the behavior of $\hat{N}$, until a level of $E_0\approx2$ keV is reached at 900 K. A decrease in E_0 is again observed during further cooling to room temperature. However, it is more continuous than what was observed for $Fe_{82}B_{12}Si_6$. After the heating cycle shown in Fig. 3 an attempt was made to remove the defects thought to be responsible for the low level of E_0 after crystallization. The annealing was done *in situ* above 1000 K for 1 h, and the specimen was slowly cooled to room temperature, where L_+ and $\hat{N}$ were measured. The results are shown in both parts of Fig. 3 (solid circles). A considerably higher level of E_0 (3000±130 eV) corresponding to $L_+=260\pm20$ Å was indeed observed, which represents a lower bound for the reference level for a defect-free specimen. E_0 is still much smaller than, e.g., in pure Ni, $E_0\approx8$ keV (see Table I). Using $E_0=3$ keV for the defect-free reference and $\lambda_{\text{free}}=8.3\times10^9$ sec^{-1} (Ref. 16) we obtain in the initial state a value of $\kappa_{\text{eff}}=2.5\times10^{12}$ sec^{-1}.

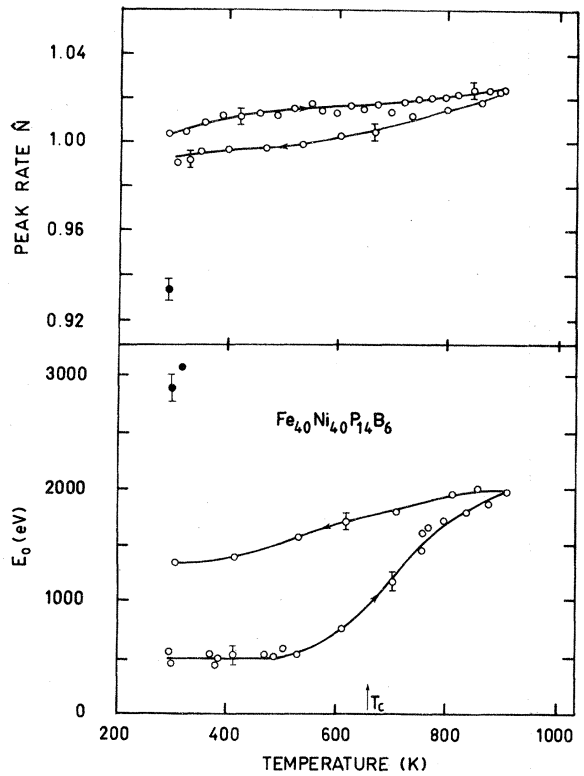

FIG. 3. Lower part: E_0 vs temperature in amorphous $Fe_{40}Ni_{40}P_{14}B_6$. $T_c=650$ K is the crystallization temperature. Solid circles: measured at room temperature after annealing at 1000 K for 1 h. Upper part: peak counting rate $\hat{N}$ vs temperature (Ref. 48). Solid circles: measured at room temperature after 1-h anneal at 1000 K (Ref. 48).

It is now possible to estimate the concentration of defects from Eq. (4). The assumption of no detrapping at room temperature leads to a lower limit of the total positron trapping probability (in units of sec^{-1})

$$\kappa_{\text{tot}}=\sum_i k_i\geq2.5\times10^{12}$$

in the amorphous state. To obtain the corresponding defect concentrations c_i ($c_i=\kappa_i/\mu_i$, Ref. 33) the specific trapping rates μ_i are needed. However, they are neither experimentally nor theoretically known. Furthermore, the diffusion-length measurements are not defect specific, whereas the conventional positron-annihilation experiments, the positron lifetime, and Doppler-broadening measurements are, to some extent, sensitive to the type of open-volume defects. The structural defects expected to exist in the amorphous structure are micrograin boundaries derived in the early microcrystalline models,[1] Bernal holes in the model of dense random packing of hard spheres (DRPHS),[38] or quasi-dislocation dipoles.[39] In the following we propose lower limits for the defect concentration using the three different structural theories. In each case we consider an upper limit for the specific trapping rate being the corresponding value obtained in crystalline metals. Our argument is based on the assumption that the defects in some amorphous metals are thought to

have low binding energies for positrons and the specific trapping rates are known to increase roughly linearly with the binding energy.[40] Recent angular correlation measurements in $Ca_{50}Al_{50}$ indicate that the positrons can be localized as strongly as is the case of monovacancies in Al.[19]

For monovacancies in crystalline metals the specific trapping rates are generally on the order of 10^{+14} to 10^{+15} sec^{-1} with binding energies ranging from 0.5 to 3.5 eV.[33] The reversible increase in E_0 (starting around 500 and 600 K in Figs. 2 and 3, respectively) can be associated with thermal detrapping of positrons from the localized states [cf. Eq. (4)]. Thus the binding energy of positrons into those defects is likely to be around 0.1—0.3 eV.[41,42] The gradual increase of E_0 would also indicate that there are many different traps having different binding energies. If the positron trapping centers are point defects, such as Bernal holes in the DRPHS model, then the specific trapping rates can be estimated to be on the order of $\mu_i \approx 10^{+13}$ to 10^{+14} sec^{-1}. Arbitrarily fixing $\mu_i \simeq 10^{14}$ sec^{-1} we have for the defect concentration in the as-received state $c_{vac} \geq 2.5\%$. Using instead the concept of line defects (quasi-dislocations) responsible for positron trapping and adopting a value of $\mu_i \approx 0.1$ $cm^2 sec^{-1}$,[33,43] a concentration of $c_{disl} \geq 2.5 \times 10^{13}$ cm^{-2} follows, which compares favorably with the estimated quasi-dislocation densities $\delta_{disl} \approx 10^{13}$ cm^{-2}.[39] In the case of grain-boundary trapping the observed tapping rate κ_{tot} corresponds[44] to an average grain size of $\bar{l} \geq 300$ Å. These estimates for the defect concentrations in various cases are collected in Table I. In all cases, the model of grain-boundary trapping (exclusively) is not consistent with the very short diffusion lengths measured in the present study.

After annealing the $Fe_{40}Ni_{40}P_{14}B_6$ specimen at 900 K E_0 was only 1300 eV at room temperature (see Fig. 3). We conclude that strong positron trapping still remains in the crystallized phase. The trapping rate can be estimated yielding $\kappa_{eff} = 1.2 \times 10^{11}$ sec^{-1} corresponding to $c_{vac} \geq 0.1\%$, $c_{disl} \geq 1 \times 10^{12}$ cm^{-2}, or $\bar{l} \leq 1400$ Å for point defects, line defects, and grain boundaries, respectively. Such a high defect concentration both before and after crystallization would result in 100% positron trapping probability in conventional fast-positron experiments. Because of the similarity of the trapping rates and binding energies before and after crystallization it is natural to expect that only very small changes in the annihilation characteristics are observed upon crystallization.[12,16,17,45] This behavior is clearly demonstrated in the peak-rate measurements presented in Fig. 3. The angular-correlation peak rate remains almost constant over the temperature range investigated with only a small hysteresis observed during cooling ($< 2\%$).

We observe further annealing of defects at 1000 K, as E_0 increases to 3000 ± 130 eV (cf. Fig. 3). However, annealing at 1000 K significantly decreases the peak rate in agreement with the present slow-positron data. This is also consistent with the observation[16] that the positron lifetime in $Fe_{40}Ni_{40}P_{14}B_6$ was $\tau \approx 160$ psec both before and after crystallization while it dropped to $\tau \approx 120$ psec after annealing for 1 h at 1073 K. The remaining defects in this crystalline alloy are likely to be grain or phase boundaries. This interpretation is supported by electron microscopy of the crystallized alloy,[46] where lamellar structures are detected with a few hundred angstroms separation distance and a grain size of the order of 1000 Å. This is in agreement with our diffusion-length estimates. Around 1000 K the annealing process results in an average grain size of a few μm.[46] Thus the diffusion length L_+ and the peak-count rate $\hat{N}$ are expected to approach the bulk values of the alloy.

D. Diffusion length in $Cu_{30}Zr_{70}$

The E_0 values measured during heat-treatment cycles for $Cu_{30}Zr_{70}$ are shown in Fig. 4 (lower curve). Our specimen and the heating scheme was similar to that used in an earlier angular correlation experiment[18,25] (300→573→300→873→300 K), the results of which are also shown in Fig. 4 (upper curve) for comparison. Our initial

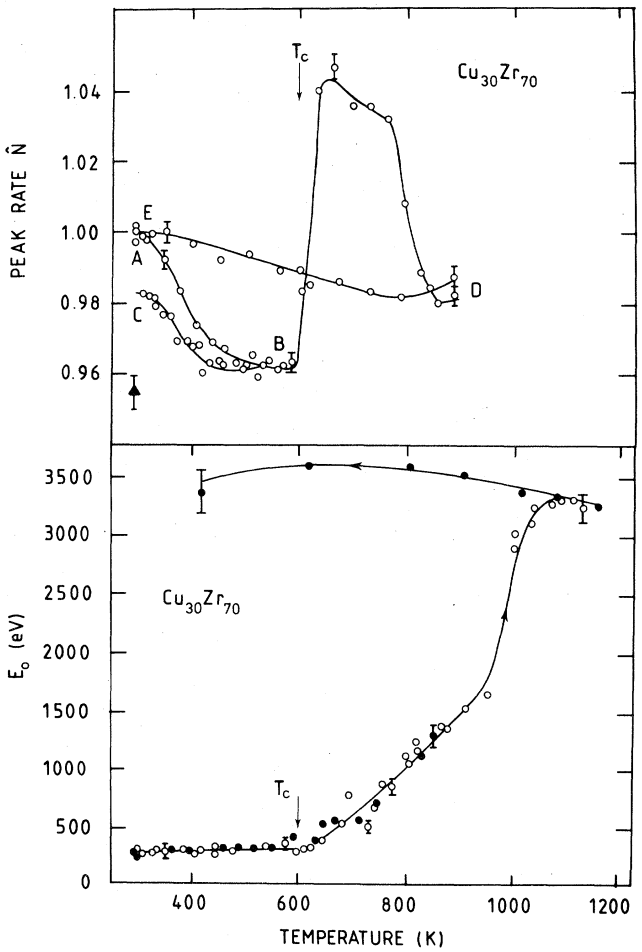

FIG. 4. Lower part: E_0 vs temperature in amorphous $Cu_{30}Zr_{70}$. The sequence of the heat treatment is 300→573→300→873→300→1160→300 K. $T_c = 600$ K and $T_m = 1280$ K (not shown) are the crystallization and melting temperatures, respectively. Open circles: temperature ascending; solid circles: temperature descending. Upper part: The peak counting rate $\hat{N}$ vs similar heat treatment $A \rightarrow E$ (open circles) (Ref. 25). Full triangle: $\hat{N}$ measured at room temperature after annealing 1 h at 1200 K (Ref. 48).

value at room temperature $E_0 = 280 \pm 40$ eV corresponding to $L_+ = 6 \pm 1$ Å is even lower than we found in the metal-metalloid glasses $Fe_{82}B_{12}Si_6$ and $Fe_{40}Ni_{40}P_{14}B_6$. From the reference value of $E_0 = 3500 \pm 150$ eV (and thus $L_+ = 360 \pm 25$ Å) obtained after high-temperature annealing we estimate the trapping rate in the as-received state $\kappa_{\text{eff}} = 2.5 \times 10^{13}$ sec^{-1}. Using similar methods of evaluating the defect densities as discussed in the preceding section, we obtain possible defect concentrations of $c_{\text{vac}} \geq 25\%$ (point defects), $c_{\text{disl}} \geq 2.5 \times 10^{14}$ cm^{-2} (dislocation-type defects), and for positrons trapped at grain boundaries an average diameter of $\bar{l} \leq 90$ Å (see Table I). These data indicate that the structure of this glass contains more open-volume regions capable of trapping positrons. A plausible explanation is the presence of the undersized boron atoms in the two previous cases, which might fill a large fraction of the open-volume areas otherwise available for positron localization.

While annealing the sample above the crystallization temperature ($T_c \approx 600$ K) Cartier *et al.*[25] found a drastic increase of the angular correlation peak counting rate $\hat{N}$, as shown in Fig. 4. It was suggested that this increase was due to the crystallization-induced formation of new defects which anneal out by 850 K causing the peak counting rate $\hat{N}$ to return to the as-received value. This was interpreted[18] as evidence that a delocalized state exists in the as-received amorphous alloy. The present results do not support this idea. During the annealing ($A \rightarrow E$; Fig. 4) E_0 stays at a very low level, increasing only slightly below T_c and more rapidly (but reversibly) above T_c. No indications of any hysteresis are seen up to 850 K. E_0 at room temperature remains unchanged from the initial value in accordance with the angular correlation results.

Both angular correlation and the positron-beam experiments are consistent with the presence of an extremely high concentration of defects capable for positron localization both in the amorphous and in the crystallized (up to 850 K) $Cu_{30}Zr_{70}$. Using the present estimates for the defect concentrations the interdefect separation becomes only a few atomic distances. This is comparable to the experimentally estimated extent of the positron wave function.[14] It is therefore possible that the positron diffusion mechanisms may be governed by interdefect tunneling processes in this material.

The drastic changes observed around T_c in the angular correlation peak count rate $\hat{N}$ can now be explained by positron localization into new phases developed during crystallization.[25] The apparent discrepancy between the two results in Fig. 4 may be due to the different implantation depths of positrons in the two experiments. It also reflects the fact that the variable-energy positron measurements described in this work, contrary to angular correlation, are insensitive to the annihilation characteristics at the localized states.

To remove the effect of positron trapping into the defects remaining after the 850-K anneal, much higher annealing temperatures were applied. An abrupt increase in E_0 is observed around 1000 K and a level of $E_0 \approx 3500$ eV was maintained during subsequent cooling to room temperature. Thus a major annealing of defects occurs at this temperature and the flatness of E_0 during cooling down suggests the existence of a delocalized positron state in the alloy. At temperatures close to the melting temperature ($T_m = 1280$ K, Ref. 47), E_0 appeared to decrease slightly. This may be an indication of positron trapping into thermally generated vacancies.[31] The sensitivity of positrons to vacancies in thermal equilibrium may be reduced by the possibility of trapping into the remaining "structural" defects. Angular correlation measurements performed after a 1200-K anneal[48] were consistent with the present data. It was observed that the peak counting rate $\hat{N}$ measured at room temperature was much lower than those found after annealing at 880 K (see Fig. 4). Amorphous $Cu_{30}Zr_{70}$ crystallizes into two separate phases having compositions of Cu—10 at.% Zr and Zr_2Cu, respectively. Moreover, the full angular correlation curve after the high-temperature anneal was very close to that for annealed Zr,[18,48] thus possibly indicating that positrons are annihilating preferentially in a Zr-rich region.

It is interesting to note that the annealed reference value of $E_0 = 3500$ eV corresponds to a positron diffusion coefficient of $D_+ \approx 0.1$ cm^2/sec, which is slightly less than the values found for annealed metals (0.3—1.5 cm^2/sec). Although very little experimental data exist for positron dif-

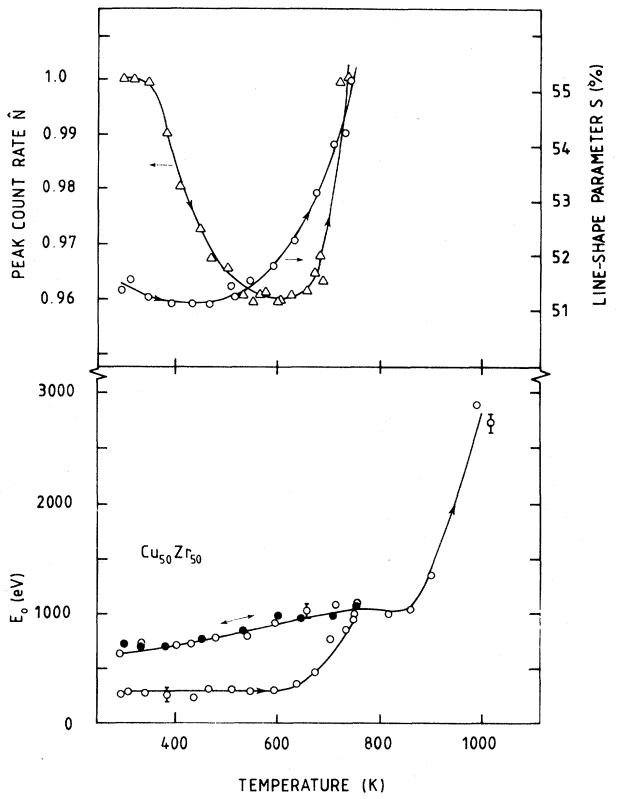

FIG. 5. Lower part: E_0 vs temperature in amorphous $Cu_{50}Zr_{50}$. The heat-treatment cycle is 300→750→300→1000 K. $T_c = 720$ K is the crystallization temperature and $T_m = 1160$ K is the melting temperature. Open circles: temperature ascending; solid circles: temperature descending. Upper part: Peak counting rate $\hat{N}$ vs temperature during initial heating of $Cu_{50}Zr_{50}$ (triangles). The line-shape parameter S of the 511-keV annihilation line recorded simultaneously with the E_0 data during initial heating of the specimen (circles).

fusion in alloys, present results indicate that at room temperature the positron-impurity scattering does not play a crucial role.

E. Diffusion length in $Cu_{50}Zr_{50}$

Figure 5 shows the E_0 values in a $Cu_{50}Zr_{50}$ metallic glass. The as-received value is again low; $E_0=270\pm40$ eV corresponding to $L_+=6\pm1$ Å. In the vicinity of crystallization at $T_c=720$ K (Ref. 49) an irreversible change in E_0 occurs, and further cooling to room temperature reduces it only slightly. Heating the specimen again shows no hysteresis. A strong increase in E_0 occurs at about 950 K and continues up to 1020 K in a similar way to what was observed for $Cu_{30}Zr_{70}$ (Fig. 4). Assuming that the reference level of E_0 is identical to that found in $Cu_{30}Zr_{70}$ (3500 eV) we obtain trapping rates close to those for the previous sample (see Table I). The structural changes seen as an increase in E_0 in Fig. 5 seem to occur in two steps (at around 720 K and above 900 K). This type of process was also observed using differential scanning calorimetry,[50] where it was argued that the crystallization into CuZr proceeds via a metastable phase formed at ≈ 720 K.

We attempted to couple the observed changes in E_0 to the angular correlation peak counting rate $\hat{N}$, measured using a similar specimen,[18] by recording the line-shape parameter S (Ref. 3) during the initial heating of the $Cu_{50}Zr_{50}$ sample. A fixed-positron-beam energy ($E=5.5$ keV) was used so that the influence of positronium formation at the surface was very small ($F<5\%$). The extracted S values represent positrons annihilating predominantly in the bulk material. Figure 5 shows both $\hat{N}$ (Ref. 18) and the S values that were measured simultaneously with the Ps fraction data (E_0 in Fig. 5) up to 700 K. While $\hat{N}$ decreases much stronger than S around 400 K, heating above 600 K causes the measured $S\approx51\%$ to increase strongly (to $S\approx55\%$) in agreement with the angular correlation measurements. However, we noticed above 700 K that S was significantly dependent on the incident positron energy in the range of 5—8 keV. The sample was cooled to room temperature during which the positron diffusion length was measured (solid circles in Fig. 5), and we then measured both F and S as a function of the incident-beam energy. The results are shown in Fig. 6. The solid line for $F(E)$ is the result of the nonlinear fit to Eq. (2) yielding $E_0=600\pm50$ eV. However, the $S(E)$ values are not proportional to $F(E)$; the shapes of the two curves are markedly different. The line-shape parameter does not saturate to a bulk value characterizing the structure of the specimen even with the highest incident energies used ($E\approx8$ keV). A fit of the $S(E)$ data to an expression analogous to Eq. (3) gives an apparent value of $E_0\approx3500$ keV. This value seems to point towards much smaller defect concentrations when compared with those shown in Table I.

Similar line-shape parameter measurements utilizing a variable-energy positron beam have recently been reported[20,51] in some amorphous metals at room temperature. The E_0 values and the general behavior of $S(E)$ obtained were in fact very similar to our results. For a $Ni_{76}Si_{12}B_{12}$ sample, for example, a value of $E_0=3.68$ keV was obtained.[20] It is interesting to note that in spite of the much higher E_0 values obtained from the line-shape measurements (as compared to the Ps fraction data), Kögel and Triftshäuser[20] estimated very similar trapping rates and defect concentrations to those shown in Table I. The reason for this apparent agreement is their use of a much higher "defect-free" reference value for E_0 (8.28 keV), which they measured for a well-annealed Ni crystal. On the basis of our annealing results, however, it seems unlikely that the diffusion length in well-annealed crystallized alloys would be so high.

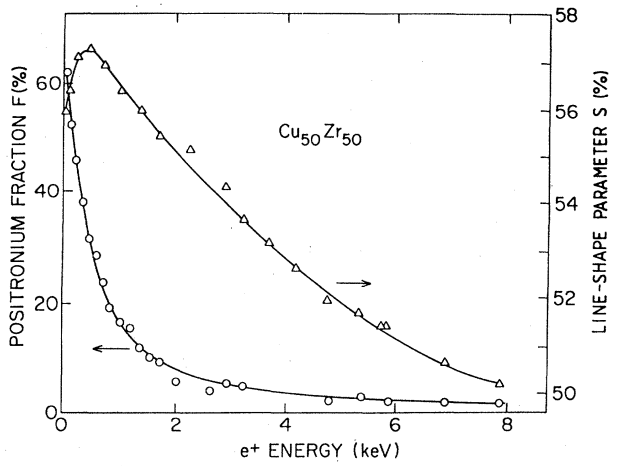

FIG. 6. The fraction F of positronium emission and the line-shape parameter S of the Doppler-broadened annihilation line as a function of the incident positron energy in the $Cu_{50}Zr_{50}$ alloy. The sample has been heat treated at 750 K and cooled to room temperature (see Fig. 5). The different shape of the curves suggests that the structure of the specimen is strongly dependent on the distance from the surface up to depths of at least 1500 Å.

The reason for the different dependence of S and F on the incident positron energy is not clear. One would expect, and indeed it is true for well-annealed nickel and silicon, that both methods should yield very similar values of E_0 (Ref. 20 and unpublished data). Based on the assumption of a spatially homogeneous sample composition and structure, a simple diffusion model predicts the same energy dependence for both.[21,51] The large discrepancy between the shapes of $S(E)$ and $F(E)$ curves in Fig. 6 suggests that the specimen is inhomogeneous as a function of the depth from the surface. Since the type and concentration of open-volume defects is the key factor in determining the shape of the annihilation line, we conclude that an inhomogeneous defect profile exists within the sample. Various reactions occurring during crystallization, like the precipitation process and densities of the crystal nucleation sites, may be affected by the presence of the surface. Alternatively, it may reflect the inhomogeneous structure of the sample in the amorphous state.

F. Diffusion length in $Gd_{67}Co_{33}$

Our deduced values of E_0 during annealing of $Gd_{67}Co_{33}$ are shown in Fig. 7. The initial value of E_0 is again very low ($E_0=390\pm60$ eV with $L_+=8\pm2$ Å), which we ascribe to positron trapping into structural defects. During the initial heating (curve *a*) E_0 remains roughly constant

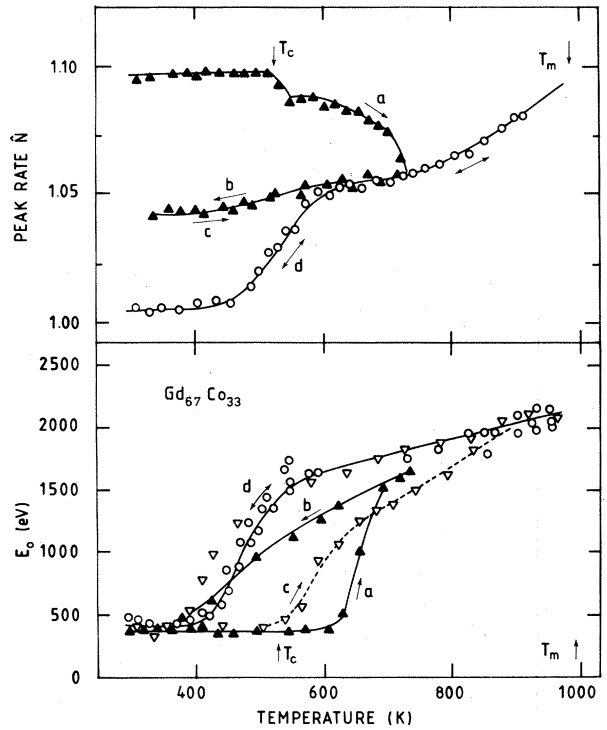

FIG. 7. Lower part: E_0 vs temperature in amorphous $Gd_{67}Co_{33}$. The heat-treatment cycle is $a \rightarrow d$. $T_c = 513$ K and $T_m = 983$ K are the crystallization and melting temperatures, respectively. Upper part: The angular correlation peak counting rate $\hat{N}$ during a similar heat-treatment cycle (Refs. 25 and 48).

until it increases strongly above 600 K. Structural change caused by the crystallization process is signaled by the different behavior of E_0 (curve *b* in Fig. 7) during cooling down to room temperature. However, E_0 resumes its original value at 300 K. Further annealing (curve *c*) to 960 K (the melting point of the material is $T_m = 983$ K) (Ref. 47) results in a reversible curve *d*, which shows a small hysteresis (≈ 10 °C) during a number of subsequent cooling and heating cycles done at approximately 0.5 °C/min. Indications of a slightly larger hysteresis phenomenon in E_0 were found using higher (> 1 °C/min) heating and cooling rates.

In this alloy we fail to obtain a high level of E_0 at room temperature, which indicates that positrons always annihilate in localized regions of the sample at 300 K. In fact, E_0 stays close to the initial value (390 eV) even after several hours of annealing at 960 K. Taking 2200 eV as a lower limit for the "defect-free" reference level, we obtain $\kappa_{\text{eff}} \geq 1.5 \times 10^{12}$ sec^{-1} corresponding to $c_{\text{vac}} \geq 1.5\%$ (vacancy-type traps), $c_{\text{disl}} \geq 1.5 \times 10^{13}$ cm^{-2} (line defects), or $\bar{l} \leq 380$ Å (grain-boundary trapping) in the as-received state at room temperature (see Table I).

The reason for the low E_0 at room temperature after annealing (curved) could be the existence of defects (e.g., grain boundaries), which we are unable to remove by annealing at 960 K. An alternate explanation could be based on a different positron chemical potential between the two existing phases (Gd_xCo and Gd_3Co, Ref. 52) which would allow the positron to reduce its zero-point energy by moving into (preferentially) one of the phases. After the present experiments transmission and scanning electron micrographs were taken of the $Gd_{67}Co_{33}$ sample at 300 K. As expected from the phase diagram[51] two different phases were observed with size distributions ranging from 0.5 to 2 μm. In addition, lamellar substructure within one of the phases was detected, with unit dimensions on the order of 1000 Å. X-ray diffraction measurements were also performed in the amorphous and annealed specimens. While diffraction peaks were not observed in the first case, only three peaks (with relatively low intensity) were detected in the crystallized alloy. The structures of the two phases expected (Gd_3Co and Gd_xCo) could not be identified because of the small number of diffraction peaks.

Angular correlation studies with similarly prepared samples and heat treatments reported earlier[25] are also shown in Fig. 7. A very small decrease in the peak counting rate $\hat{N}$ is observed at the crystallization temperature followed by a slightly larger decrease around 700 K (curve *a*). Cooling from 740 K results in an almost-temperature-independent branch *b*, which is reversible (curve *c*). A reversible behavior (curve *d*) is seen after a 900-K anneal similar to the present results. The peak counting rate $\hat{N}$ is smallest at room temperature and it increases in a sigmoidal way similar to the E_0 data up to 900 K. The major difference between the two experiments is a shift in temperature of about 60 °C. This change in the mean value of the sigmoidal part of the curve may be ascribed to the different heating rates between the two experiments. To check the possibility of positron localization in one of the two phases angular correlation peak rate $\hat{N}$ was measured[48] for the nominally single-phase material Gd_3Co (< 2 mol % Gd_xCo). $\hat{N}$ was observed to increase much stronger than in annealed metals but weaker than in the crystallized $Gd_{67}Co_{33}$ specimen in the temperature range 500–750 K, and the shape of $\hat{N}$ versus temperature was sample dependent. Thus we can argue that a residual second phase is still present in the samples capable for positron trapping.

An increased peak counting rate $\hat{N}$ is normally attributed to a higher positron trapping rate. This would imply that the angular correlation results completely contradict the present data. From the angular correlation results it was concluded[25] that a delocalized positron state exists at room temperature, and the *S*-shaped increase in $\hat{N}$ centered at 530 K is due to positron trapping at thermally generated monovacancies in this alloy. Application of the standard trapping model[33] yielded a monovacancy formation energy of $E_{1v}^F = 0.63 \pm 0.08$ eV. Our results indicate not only very high trapping at room temperature, but also show that significant positron trapping remains at higher temperatures after the sigmoidal increase in E_0. We can estimate the trapping rate to be $\kappa_{\text{eff}} \geq 2 \times 10^{10}$ sec^{-1} at 600 K.

One straightforward explanation to resolve the discrepancy between the two results is to assume that all positrons are trapped predominantly into low-binding-energy traps at room temperature with annihilation characteristics similar to a delocalized positron state in

the crystalline alloy. Above 400 K positrons are thermally detrapped from the shallow traps and still have a high probability to be localized into a lower concentration of deeper positron traps. Fitting the sigmoidal increase of E_0 to the model of thermal detrapping of positrons[22] a positron-defect binding energy of 0.7 ± 0.06 eV is obtained. Thus the total trapping probability decreases resulting in an increase in E_0, while the angular correlation curve, reflecting the annihilation characteristics of deeper positron traps, becomes narrower. However, this cannot explain the temperature hysteresis found on this system.

Another mechanism to account for the increased positron trapping with temperature could be precipitation or phase-separation phenomena. The phase diagram of Gd-Co system at 67 at.% Gd assumes a mixture of two phases ($CoGd_x$ and $CoGd_3$) at room temperature. If a miscibility gap between the two phases exists, then the relative fractions of the phases as well as the area of the phase boundaries depend both on sample temperature and on heating and cooling rates of the specimen. This can account for the hysteresis phenomena observed in the positron diffusion length and the temperature shift of the sigmoidal increase of $\hat{N}$ and E_0 in Fig. 7. The large change in $\hat{N}$ versus temperature that is observed in Fig. 7 is associated with the different momentum spectra observed from the two different phases (see Fig. 1 in Ref. 18). The angular correlation results after water quenching from 880 K (Ref. 18) can also be understood in the context of this model, since the high-temperature thermal-equilibrium phases are not obtained during the rapid quench.

No signs of thermal vacancy trapping in this material were observed, even through the diffusion length was measured up to 50 °C from the melting temperature. This is likely due to competing positron trapping into a much higher concentration of defects that are not removable by annealing.

V. CONCLUSIONS

We have measured the temperature dependence of the effective positron diffusion length in various metallic glasses with a variable-energy positron beam. In the as-received state an extremely short diffusion length ($L_+ \approx 10$ Å) sensitive to the type of the specimen was observed, which is more than 2 orders of magnitude smaller than that in annealed crystalline metals. We ascribe this to positron trapping into open-volume defects inherently present in the amorphous structure. The defect density in the metal-metalloid glasses is generally lower than in the metal-metal glasses. This is thought to be due to the presence of undersized boron atoms, which partially fill the open-volume areas otherwise capable of localizing positrons. We show evidence that the binding energy of positrons into these defects is relatively small, resulting in positron thermal detrapping in the amorphous phase. Although our measurements cannot provide conclusive information on the nature of these defects, the present data are consistent with a variety of different traps some of which may be Bernal holes of the DRPHS model with a concentration of the order of 1%. Alternatively, an equivalent line-defect (quasi-dislocation) concentration around 10^{13} cm^{-2} would fit our data. A simple model of micrograin boundary trapping of positrons could not be made to fit the results with physically reasonable parameters.

Heating the specimen below the crystallization temperature causes both reversible and irreversible changes in the positron diffusion length. They are considered to be due to thermal detrapping from the low-binding-energy defects and structural relaxation of the amorphous structure, respectively. A crystallization of T_c causes gradual changes in the trapping rate with a different temperature-dependent behavior. Annealings several hundred degrees above T_c are needed to reduce the trapping rates significantly in most specimens. Annealing close to the melting point results in a positron state with a degree of localization highly dependent on the particular glass. Both amorphous and crystalline phases contain a spectrum of different positron traps with varying binding energies. Very little evidence of thermal generation of vacancies is observed. Our measurements also show strong indications of an inhomogeneous defect profile near the surface of a crystallized alloy, suggesting that the presence of the surface affects the crystallization and precipitation processes, or reflecting the inhomogeneous structure of the as-prepared amorphous metal.

ACKNOWLEDGMENTS

We are indebted to M. Carroll, J. Hurst, and A. Moodenbaugh for technical support. One of us (A.V.) thanks his colleagues for the hospitality during his visit at Brookhaven National Laboratory (BNL). Work performed at BNL is supported by the Division of Materials Sciences, U. S. Department of Energy, under Contract No. DE-AC02-76CH00016.

*Permanant address: Laboratory of Physics, Helsinki University of Technology, SF-02150 Espoo 15, Finland.

[1]For a review, see, e.g., *Glassy Metals I,* Vol. 461 of *Topics in Applied Physics,* edited by H.-J. Güntherodt and H. Beck (Springer, Berlin, 1981).

[2]*Point Defects and Defect Interaction in Metals,* edited by J. Takamura, M. Doyama, and M. Kiritani (University of Tokyo Press, Tokyo, 1982).

[3]*Positron Annihilation,* edited by P. G. Coleman, S. C. Sharma, and L. M. Diana (North-Holland, Amsterdam, 1982).

[4]N. Shiotani, in *Positron Annihilation,* Ref. 3, pp. 561–572.

[5]P. Hautojärvi and J. Yli-Kauppila, Nucl. Instrum. Methods 199, 75 (1982).

[6]Z. Kajcsos, T. Kemény, and G. Bramer, Nucl. Instrum. Methods 199, 373 (1982).

[7]H. S. Chen and S. Y. Chuang, Phys. Status Solidi A 25, 581 (1974).

[8]M. Doyama, S. Tanigawa, K. Kuribayashi, H. Fukushima, K. Hinode, and F. Saito, J. Phys. F 5, L230 (1975).

[9]S. Y. Chuang, S. J. Tao, and H. S. Chen, J. Phys. F 5, 1681 (1975).

[10]S. Tanigawa, K. Hinode, R. Nagai, K. Kaube, M. Doyama, and N. Shiotani, Phys. Status Solidi A 51, 249 (1979).

[11]S. Y. Chuang, P. K. Tseng, G. J. Jan, and H. S. Chen, Phys.

Status Solidi A 48, K181 (1978).
[12]R. H. Howell and R. W. Hopper, Scr. Metall. 13, 367 (1979).
[13]Z. Kajcsos, J. Winter, S. Mantl, and W. Triftshäuser, Phys. Status Solidi A 58, 77 (1980).
[14]N. Shiotani, N. Sakai, H. Sekigawa, and T. Mizoguchi, J. Phys. Soc. Jpn. 50, 828 (1980).
[15]J. Yli-Kauppila, P. Moser, H. Künzi, and P. Hautojärvi, Appl. Phys. A 27, 31 (1982).
[16]P. Moser, P. Hautojärvi, J. Yli-Kauppila, and C. Corbel, Radiat. Eff. 62, 153 (1982).
[17]S. Tanigawa, K. Shima, H. Iriyama, and Y. Waseda, in *Positron Annihilation,* Ref. 3, 584–586.
[18]E. Cartier, F. Heinrich, M. Küng, and H.-J. Güntherodt, Nucl. Instrum. Methods 199, 147 (1982).
[19]E. Cartier, F. Heinrich, M. Küng, and H.-J. Güntherodt, in *Positron Annihilation,* Ref. 3, pp. 573–575.
[20]G. Kögel and W. Triftshäuser, in *Positron Annihilation,* Ref. 3, pp. 595–598.
[21]For a review, see lecture notes of A. P. Mills, Jr. and K. G. Lynn, in *Positron Solid State Physics,* edited by W. Brandt and A. Dupasquier (North-Holland, Amsterdam, 1983).
[22]P. J. Schultz, K. G. Lynn, R. N. West, C. L. Snead, Jr., I. K. MacKenzie, and R. W. Hendricks, Phys. Rev. B 25, 3637 (1982).
[23]A. Vehanen, K. G. Lynn, P. J. Schultz, A. N. Goland, C. L. Snead, Jr., H.-J. Güntherodt, and E. Cartier, in *Positron Annihilation,* Ref. 3, pp. 587–589.
[24]Supplied by Allied Corporation, Morristown, NJ 07960.
[25]E. Cartier, F. Heinrich, and H.-J. Güntherodt, Phys. Lett. 81A, 393 (1981).
[26]K. G. Lynn and H. Lutz, Rev. Sci. Instrum. 51, 977 (1980).
[27]A. P. Mills, Jr. and R. J. Wilson, Phys. Rev. A 26, 490 (1982).
[28]A. P. Mills, Jr., P. M. Platzman, and B. L. Brown, Phys. Rev. Lett. 41, 1076 (1978).
[29]A. P. Mills, Jr., Phys. Rev. Lett. 41, 1828 (1979).
[30]K. G. Lynn, Phys. Rev. Lett. 43, 391 (1979).
[31]K. G. Lynn and H. Lutz, Phys. Rev. B 22, 4143 (1980).
[32]A. P. Mills, Jr., Solid State Commun. 31, 623 (1979).
[33]R. M. Nieminen and M. J. Manninen, in *Positrons in Solids* Vol. 12 of *Topics in Current Physics,* edited by P. Hautojärvi (Springer, Berlin, 1979).
[34]B. Bergersen, E. Pajanne, P. Kubica, M. J. Stott, and C. H. Hodges, Solid State Commun. 15, 1377 (1974).
[35]Note that κ_{eff} can be calculated without knowing the value of D_+ (and A) if the defect-free reference value for E_0 is known.
[36]J. R. Cost and J. T. Stanley, Scr. Metall. 15, 407 (1981).
[37]J. L. Walter, P. Rao, E. F. Koch, and S. F. Bartram, Metall. Trans. 8A, 1141 (1977).
[38]For a recent review, see R. W. Cahn, Contemp. Phys. 21, 43 (1980).
[39]H. Kronmüller, J. Phys. (Paris) Colloq. 8, C-618 (1980).
[40]R. M. Nieminen and J. L. Laakkonen, Appl. Phys. 20, 181 (1979).
[41]M. J. Manninen and R. M. Nieminen, Appl. Phys. A 26, 93 (1981).
[42]P. Hautojärvi, J. Johansson, A. Vehanen, J. Yli-Kauppila, J. Hillairet, and P. Tzanétakis, Appl. Phys. A 27, 49 (1982).
[43]L. C. Smedskjaer, M. Manninen, and M. J. Fluss, J. Phys. F 10, 2237 (1980).
[44]B. T. A. McKee, G. J. C. Carpenter, J. F. Watters, and R. J. Schultz, Philos. Mag. A 41, 65 (1980).
[45]T. Mihara, S. Otake, H. Fukushima, and M. Doyama, J. Phys. F 11, 727 (1981).
[46]R. S. Tiwari, S. Ranganathan, and M. V. Heimendahl (unpublished).
[47]M. Hansen, *Constitution of Binary Alloys* (McGraw-Hill, New York, 1958).
[48]E. Cartier, unpublished data.
[49]R. L. Freed and J. B. Vander Sande, J. Noncryst. Solids 27, 9 (1978).
[50]W. Triftshäuser and G. Kögel, in *Positron Annihilation,* Ref. 3, pp. 142–152; W. Triftshäuser and G. Kögel, Phys. Rev. Lett. 48, 1741 (1982).
[51]K. H. J. Buschow and A. S. Van der Goot, J. Less-Common Metals 17, 249 (1969).